

# Global Lineaments and Ring Structures: Application of Digital Terrain Modelling

Igor V. Florinsky

Institute of Mathematical Problems of Biology  
Russian Academy of Sciences  
Pushchino, Moscow Region, 142290, Russia  
[iflor@mail.ru](mailto:iflor@mail.ru)  
Phone/fax: +7-4967-732408 / 330570

**Abstract:** *At the global scale, a comprehensive quantitative analysis of the topography may be essential for improvement of existing tectonic models, and may give a clearer insight into the evolution of the Earth. The objective of this study was to detect and interpret hidden, topographically expressed global linear and circular structures using methods of digital terrain modelling. The study was based on a 30 arc-minutes gridded global digital elevation model (DEM). Eighteen local and regional topographic variables were for the first time calculated and mapped for the entire surface of the Earth including both land and seafloor relief. The following variables were derived from the smoothed DEM: twelve curvatures (horizontal, vertical, accumulation, difference, ring, minimal, maximal, mean, Gaussian, unsphericity, horizontal excess, and vertical excess curvatures), slope, aspect, rotor, specific catchment area, specific dispersive area, and accumulation zones. Global maps of these attributes were successfully analysed to reveal spatial curvilinear and circular structures. First, five double helical structures were detected. The structures are topographically expressed by patterns of the global watershed and ridge network on maps of specific catchment area. They are apparently associated with traces of the torsional deformation of the planet: two double helices are in reasonable agreement with theoretically predicted traces of shear fractures, while other two double helices – with theoretical traces of cleavage cracks. Second, about fifty quasi-circular structures were detected on global maps of horizontal, vertical, minimal, maximal, and ring curvatures. Some of these features coincide with ring structures revealed previously. To avoid artefacts due to distortion of map projections, the stereographic projection should be used for global maps of topographic variables intended to reveal ring structures. Analysis of global maps of topographic attributes can be useful to study other problems of geology and geophysics.*

**Keywords:** Tectonics; geological structure; curvature; catchment area; helix; planet.

---

## 1. Introduction

Relief is one of the main characteristics of a planet. Resulting from the interaction of various endogenous and exogenous geophysical processes of different spatial and temporal scales, topography carries information on both surface processes and tectonic features (Ollier, 1981; Burbank & Anderson, 2000; Scheidegger, 2004). Thus, it is not surprising that global digital elevation models (DEMs) are used in the Earth and planetary science: to develop a mantle convection model of the Earth (Cazenave et al., 1989), to study global terrestrial hydrological processes (Coe, 1998; Renssen & Knoop, 2000), to explore geomorphometric characteristics of the Earth (McClean & Evans, 2000; Vörösmarty et al., 2000; Kazanskii, 2005), to refine models of the shape and the interior structure of the Moon (Smith et al., 1997), to study global tectonic and surface processes on Mars (Smith et al., 1999; Phillips et al., 2001), and to map non-spheroidal small celestial bodies (Nyrtsov, 2000).

There are geological, geophysical, and geomorphic evidences contradicting the plate-tectonic theory (Pavlenkova, 1995; Smoot, 1997, 2001; Pratt, 2000). To link those evidences with ideas of continental drift, seafloor spreading, and subduction, modifications of the plate-tectonic hypothesis were proposed (e.g., Bush, 1983; Besprozvanny et al., 1994; Anderson, 2002). Also, there are alternative tectonic theories: the expanding Earth (Carey, 1988), the surge tectonics (Meyerhoff et al., 1996), the wrench tectonics (Storetvedt, 2003), and others. The diversity of tectonic paradigms is mainly associated with the lack of sufficient information about the Earth interior and the geology of past ages. A comprehensive quantitative analysis of the global topography may be essential to upgrade tectonic theories, and may give a clearer insight into the evolution of the Earth.

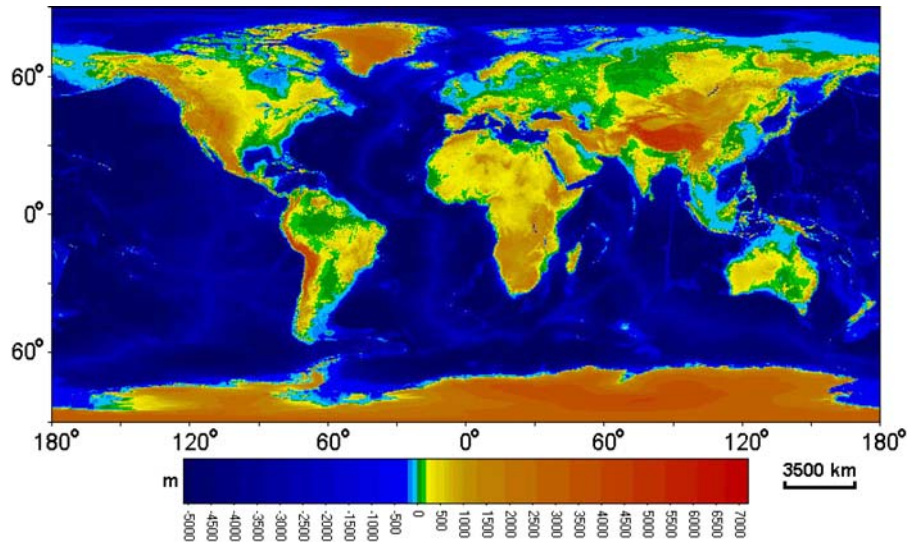


Fig. 1: Global elevation map based on the 30 arc-minutes gridded global DEM.

Among geological features, of special interest are lineaments and ring structures. These are (curvi)linear and radially concentric surficial manifestation of geological phenomena, processes, and structures of various origin, age, depth, and size (Trifonov et al., 1983). Lineaments are usually associated with faults, folds, fracture zones, seamount chains, and other linear features and their sequences. Ring structures are connected with craters, salt and mantle diapirs, volcanic and volcano-tectonic structures, etc. (Bush et al., 1987). Linear and ring structures, as a rule, are topographically expressed, and can be observed at a wide range of spatial scales. At detailed and regional scales, one can geometrically treat lineaments and ring structures as planar (straight) lines and planar isometric figures or closed curves (e.g., quasi-circles, ellipses, and ovals), correspondingly. At continental and global scales, the structures should be considered as spatial – spherical or ellipsoidal – curves and figures.

At the global scale, considerable studies have been given to both lineaments (Chebanenko, 1962; Katterfeld & Charushin, 1973; O'Driscoll, 1980; Besprozvanny et al., 1994; Poletaev, 1994; Volkov, 1995; Fedorov, 2003) and ring structures (Norman et al., 1977; Zeilik, 1978; Glukhovskiy et al., 1983; Poletaev, 1983; Ezhov & Khudyakov, 1984; Kats & Makarova, 1985; Kats et al., 1989). These works were carried out by a visual analysis of topographic, physiographic, and geological maps and remotely sensed images. The existence of global linear and circular structures, which may be expressed tectonically and topographically, is still questionable. This is because of (a) a qualitative character of maps analysed; (b) inaccurate presentation of seafloor bathymetry on the maps produced before a reasonably fair bathymetric data (Smith & Sandwell, 1997) became available; and (c) subjective nature of a visual analysis, particularly as regards lineament detection (Wise, 1982).

Digital terrain models (DTMs) were used to detect linear and circular topographic features at regional (Gosteva et al., 1983; Schowengerdt & Glass, 1983; Florinsky, 1992, 1996, 1998b; Chorowicz et al., 1999; Jordan, 2003) and continental (Moore & Simpson, 1983; Florinsky, 2005) scales. However, to this point digital terrain modelling has not been applied to study lineaments and ring structures at the global scale. The objective of this study was to detect and interpret hidden, topographically expressed global linear and circular structures using methods of digital terrain modelling (Moore et al., 1991; Florinsky, 1998a; Pike, 2000).

## 2. Materials and Methods

This study was based on a 30 arc-minutes gridded global DEM assembled using several sources (Fig. 1). Elevations of the land topography were derived from GLOBE (GLOBE Task Team et al., 1999). Most of the seafloor topography was taken from ETOPO2 (U.S. Department of Commerce, 2001). Bathymetry of the Antarctic Continental Shelf, Caspian Sea, and large lakes was digitised using topographic maps (USSR General Headquarters, 1984). The DEM consisted of 721 columns by 361 rows, viz. 260,281 points. For Antarctica and Greenland, GLOBE includes elevations of ice surfaces rather than subglacial topography (Hastings & Dunbar, 1999). These areas were included into the DEM and thereafter processed to retain a united configuration of global data. They can be ignored in the further analysis.

Previous studies of accuracy, errors, and artefacts of global DEMs (Coe, 1998; Hastings & Dunbar, 1999; Arabelos, 2000) and our preliminary experiments (Florinsky, 2005) demonstrated that the DEM includes a potent high-frequency noise. This leads to derivation of useless, noisy digital models and unreadable maps of secondary topographic variables (Florinsky, 2002). The problem can be resolved by DEM smoothing. Thus, to reduce noise in the DEM, we applied one, two, and three iterations of smoothing to the DEM using 3×3 kernel with linear inverse distance weights (Tobler, 1967).

This study was the first application of digital terrain modelling to reveal linear and circular structures at the global scale. Topographic attributes *a priori* 'effective' for this purpose were unknown. Therefore, it was reasonable to use a representative set of variables. DTMs of the following local topographic variables were derived from the smoothed DEMs: 12 curvatures (i.e., horizontal, vertical, accumulation, difference, ring, minimal, maximal, mean, Gaussian, unsphericity, horizontal excess, and vertical excess curvatures), slope, aspect, and rotor. A model of accumulation zones was also calculated. DTMs of two regional topographic variables were derived from the smoothed DEMs: specific catchment area and specific dispersive area. Definitions and formula of the variables can be found elsewhere (Florinsky, 1998a; Shary et al., 2002). Local variables were calculated by the method of Florinsky (1998b). Regional variables were calculated by a single flow direction algorithm with removing 'pits' (Martz & de Jong, 1988) adapted to spheroidal trapezoidal grids. All DTMs produced had a resolution of 30 arc-minutes.

To gain a better representation and understanding of global patterns of topographic attributes, they were mapped (Fig. 2) using natural logarithmic scales (detailed explanation can be found elsewhere – Shary et al., 2002). Additionally, specific catchment and dispersive areas were mapped with classification of their values into two levels (Fig. 3). The plate carrée projection (the equirectangular, equidistant cylindrical projection with the equator as the standard parallel – Bugayevskiy & Snyder, 1995) was used for mapping of topographic variables (Figs. 2 and 3). For convenience, shorelines are shown on most of maps, but 30° graticules are removed. DTM treatment and mapping (Figs. 1-3) was done with software LandLord 4.0 (Florinsky et al., 1995).

Maps of topographic variables (Figs. 2 and 3) were examined in detail. Attention was given to lineaments running all the globe and large quasi-circular structures. The maps represent these features by image patterns strung out along some directions and image texture. The structures detected were mapped using the plate carrée and stereographic projections with ArcView GIS 3.0 (© ESRI, 1992-1996).

### 3. Results and Discussion

#### 3.1 Global Maps of Topographic Variables

Global maps of local and regional topographic variables represent peculiarities of the Earth's mega-relief in different ways, according to physical and mathematical sense of a particular variable (detailed interpretation of the variables can be found elsewhere – Shary et al., 2002). In particular, the map of horizontal curvature (Fig. 2A) delineates areas of flow divergence and convergence (positive and negative values, correspondingly). Vertical curvature (Fig. 2B) shows areas of relative acceleration and deceleration of flows (positive and negative values, correspondingly). Positive values of minimal curvature display 'hills' (Fig. 2C), while negative values of maximal curvature – 'depressions' (Fig. 2D). Horizontal excess curvature (Fig. 2E) describes to what extent horizontal curvature is larger than minimal one. Vertical excess curvature (Fig. 2F) describes to what extent vertical curvature is larger than minimal one. Positive values of Gaussian curvature mark elliptic areas, while its negative values – hyperbolic ones (Fig. 2G). The map of rotor (Fig. 2H) delineates zones where flow lines turn clockwise and anti-clockwise (positive and negative values, correspondingly). Zero values of ring curvature (Fig. 2I) are typical for radially symmetrical landforms with vertical axes of symmetry. Combination of data on accumulation and mean curvatures allows one to portray zones of flow accumulations (Fig. 2J). Sites of fault intersections are usually associated with topographically expressed accumulation zones (Florinsky, 2000).

Maps of regional variables delineate various features of drainage and watershed networks. The map of specific catchment area (Fig. 2K) clearly displays land watersheds and oceanic ridges (black), as well as land and sea depressions (white). The map of specific dispersive area (Fig. 2L) displays land valleys and oceanic troughs (black), as well as ridges and plateaus (white). Maps of specific catchment area classified into two levels display the global watershed and ridge network (Fig. 3A-C). The greater number of the DEM smoothing, the more generalized picture of the network is observed. The map of specific dispersive area classified into two levels displays the global drainage and valley network (Fig. 3D).

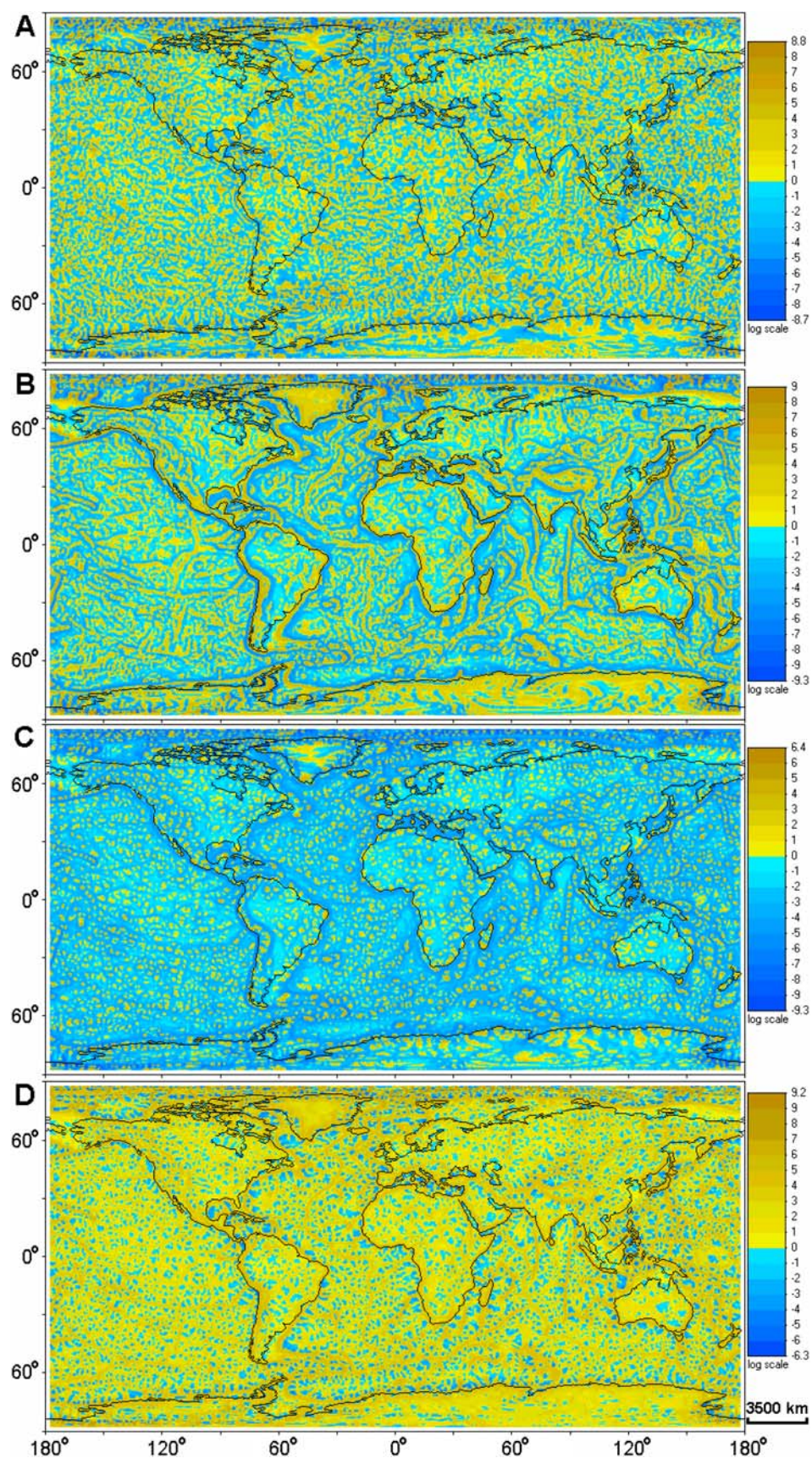


Fig. 2: Global maps of topographic variables derived from the 3-times smoothed DEM: A – horizontal curvature, B – vertical curvature, C – minimal curvature, D – maximal curvature,

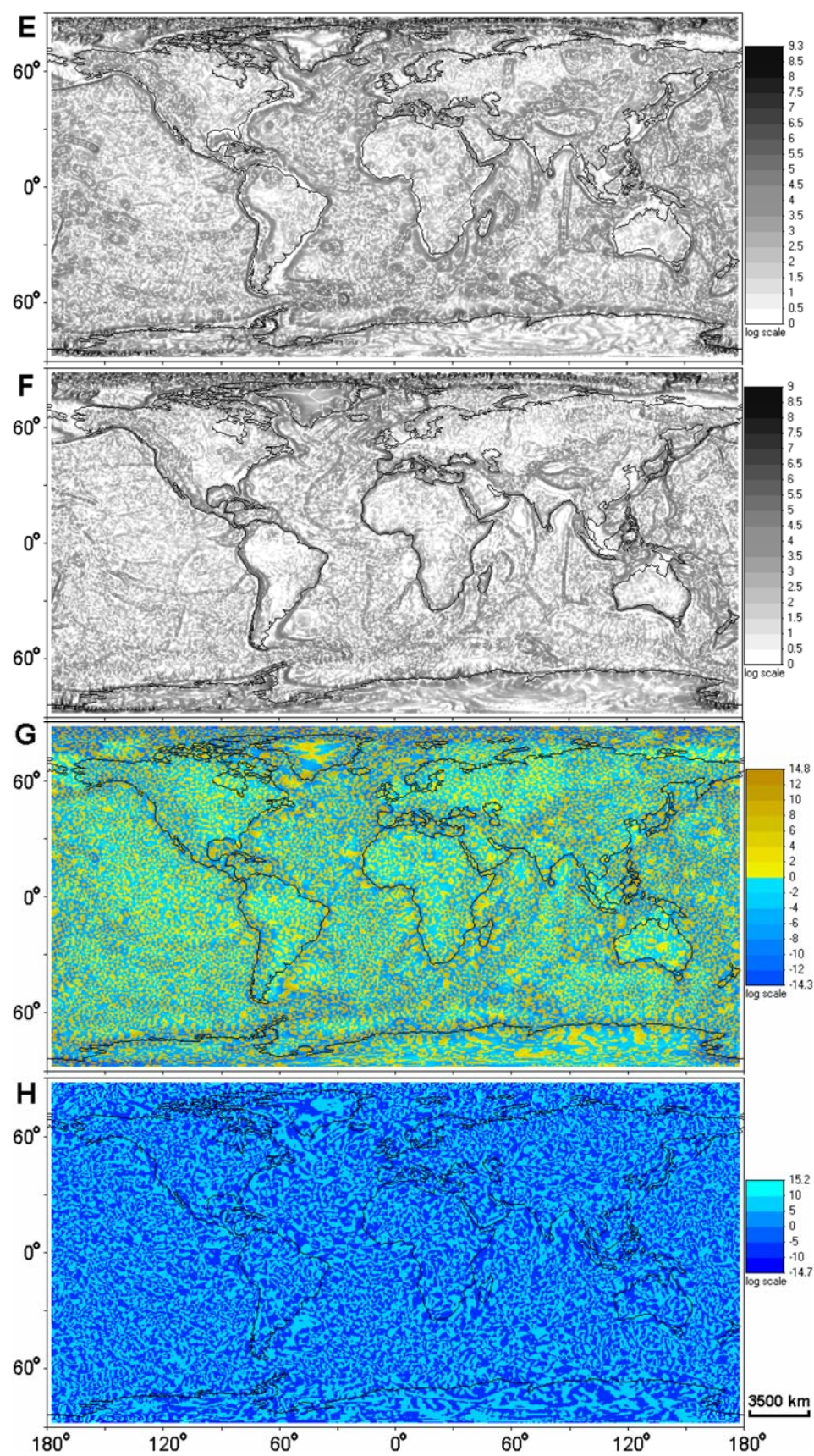


Fig. 2 (cont.): E – horizontal excess curvature, F – vertical excess curvature, G – Gaussian curvature, H – rotor,

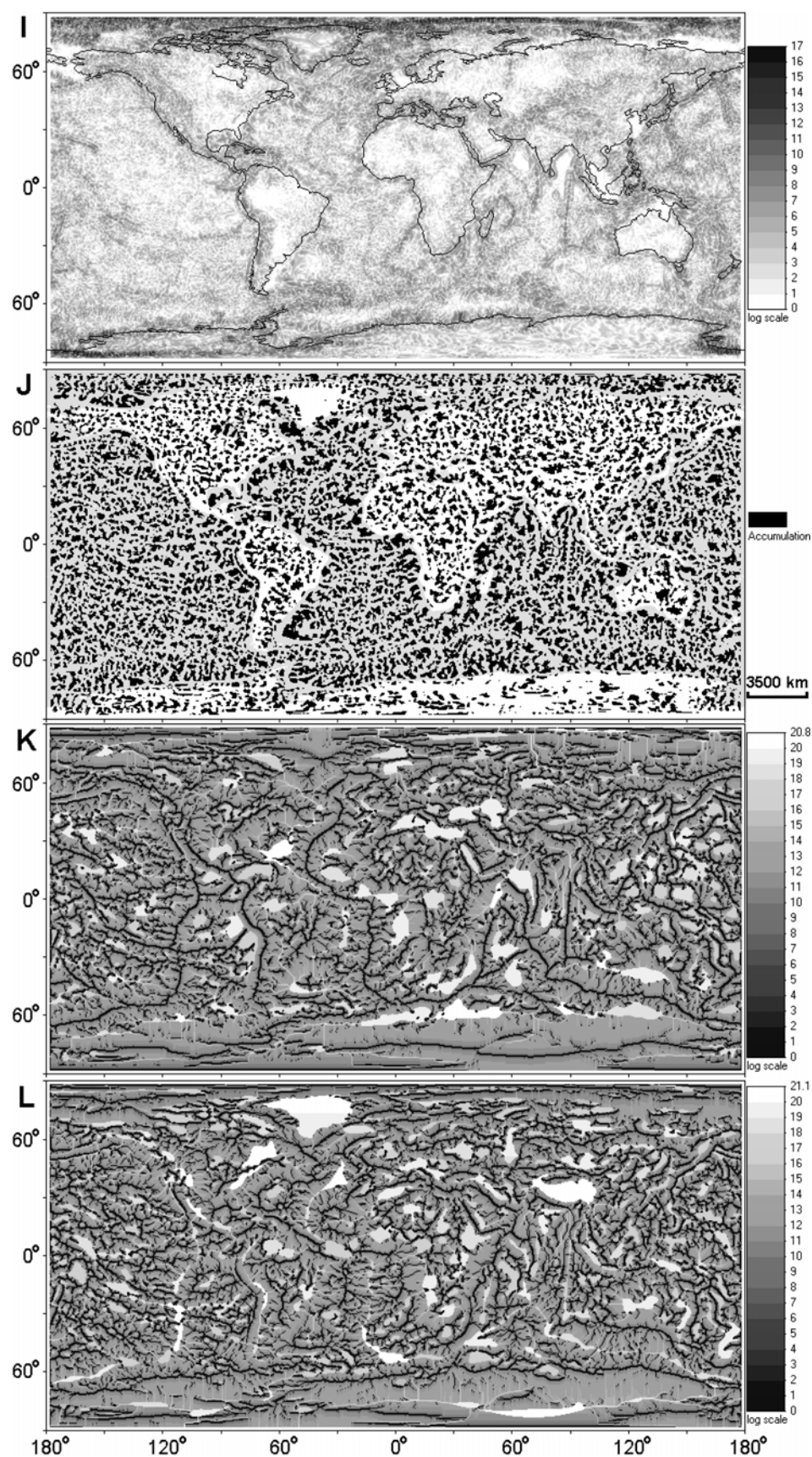


Fig. 2 (cont.): I – ring curvature, J – accumulation zones, K – specific catchment area, and L – specific dispersive area.

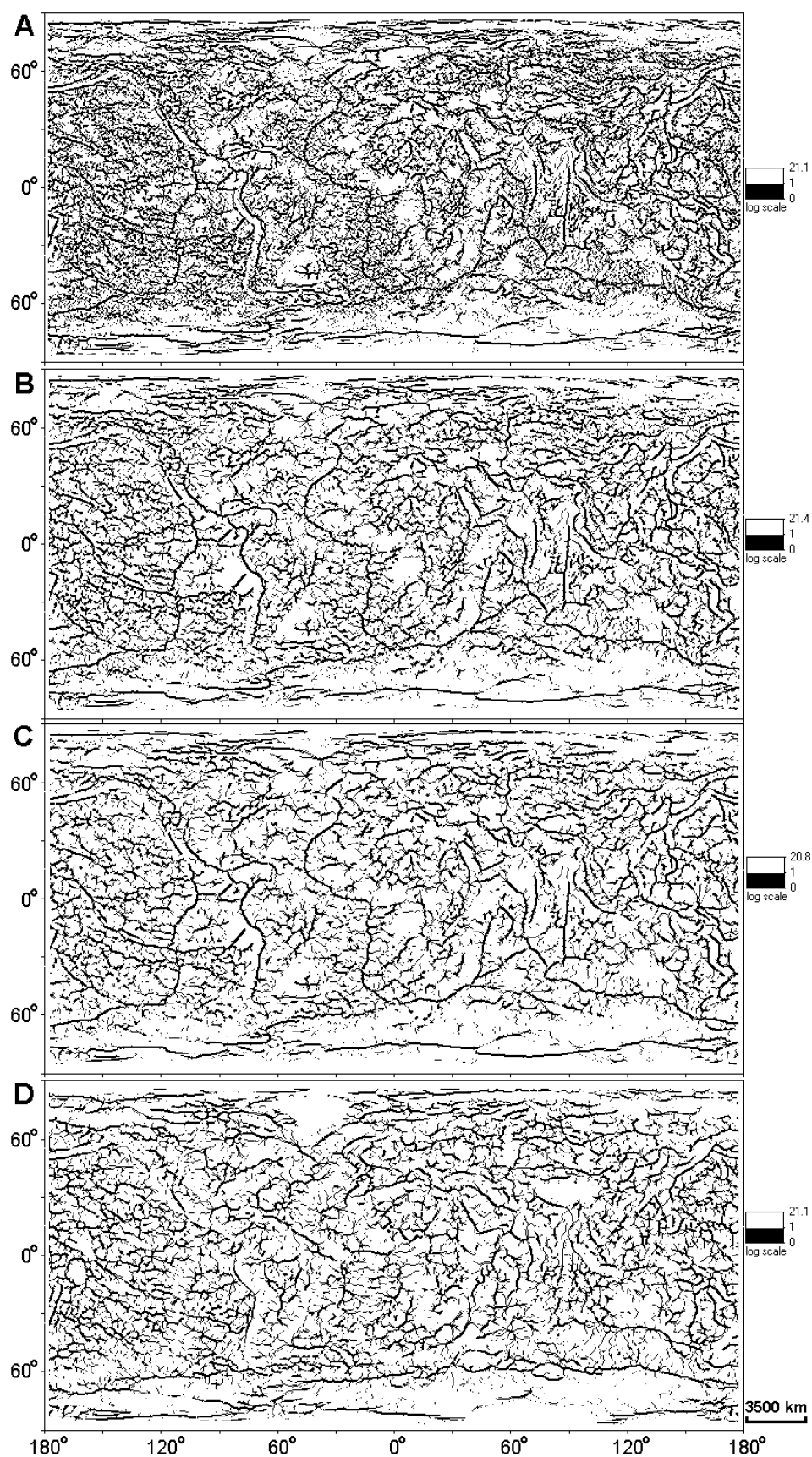


Fig. 3: Global maps of regional variables classified into two levels: A-C – specific catchment area for the 1-time smoothed DEM (A), the 2-times smoothed DEM (B), and the 3-times smoothed DEM (C); and D – specific dispersive area for the 3-times smoothed DEM.

### 3.2 Lineaments (Helices)

To detect lineaments, the variable of greatest practical utility was specific catchment area with values classified into two levels (Fig. 3A-C). I detected five mutually symmetrical pairs of global lineaments or more precisely, five double helices encircling the Earth from pole to pole (Figs. 4 and 5). The structures revealed are helical zones rather than simply lines. Each double helix is named for area(s) of intersection(s) of its arms (Table I). Arms running clockwise upward and counter-clockwise upward (dextral and sinistral helices) are called right and left arms, correspondingly.

The global lineaments revealed cannot be artefacts due to DEM errors, the DEM treatment, and the DEM grid geometry (Florinsky, 2005). First, noise and errors have usually a random distribution in DEMs. Second, smoothing and derivation of topographic variables were carried out using local filters ( $n \times n$  moving windows). Third, the grid geometry may amplify its own preferential directions: orthogonal (north-south, east-west) and diagonal (northeast-southwest, northwest-southeast). However, the structures detected have (a) the global character relative to the DEM; and (b) directions distinct from orthogonal and diagonal ones. A subjective character of the visual analysis remains the only cause of possible artefacts.

Each helical zone transgresses regions dissimilar in respect to their tectonic origin and age. The left arm of the Caucasus-Clipperton double helix is the longest helical arm revealed (Table I): it encircles the Earth nearly two times (Figs. 4A and 5A). It starts in the Beaufort Sea, crosses Greenland, the northern Atlantic basin, Eurasia (from Scotland to the East China Sea), the central Pacific basin, South America (from the Peruvian Andes to the Brazilian Highlands), the southern Atlantic basin, South Africa, the southern Indian Ocean basin (along the Southeast Indian Ridge), and disappears in the Southern Ocean basin. The right arm of the Caucasus-Clipperton structure (Figs. 4A and 5A) also starts in the Beaufort Sea. This crosses Eurasia (from the East Siberian Sea to the Apennines), the Atlas Mountains, the central Atlantic basin, the Greater Antilles, the Yucatan Peninsula, and the central Pacific basin (along the Clipperton Fracture Zone). The left arm of the Biscay-Santa Cruz double helix (Figs. 4B and 5B) starts in the Beaufort Sea too. The arm crosses the Labrador Sea, the northern Atlantic basin, the Mediterranean Sea, the Arabian Peninsula, Deccan, Bay of Bengal, New Guinea, the Southwest Pacific Basin, the East Pacific Rise, Tierra del Fuego, and ends in the Scotia Sea. The right arm of the Biscay-Santa Cruz structure (Figs. 4B and 5B) crosses Eurasia from the Taymyr Peninsula to the Iberian Peninsula, the central Atlantic basin, Cuba, the Yucatan Peninsula, the central Pacific basin, the Coral Sea, and disappears in the central Australia. The left arm of the Marcus double helix (Figs. 4C and 5C) starts northward Novaya Zemlya. This crosses Siberia, the Korean Peninsula, Japan, the Pacific Ocean basin, Tierra del Fuego, and disappears in the Scotia Sea. The right arm of the Marcus structure (Figs. 4C and 5C) starts in North America, near the Great Bear Lake. The arm crosses the Gulf of Alaska, the Pacific Ocean basin, Borneo, the Indian Ocean basin (along the Southwest Indian Ridge), and disappears in the Southern Ocean basin. The left arm of the Dakar double helix (Figs. 4D and 5D) starts in the Buffin Bay. This crosses the northern Atlantic Ocean basin, the Grain Coast of Africa, the Angola Basin, Cape of Good Hope, the Agulhas Basin, and the Enderly Plain in the Southern Ocean basin. The right arm of the Dakar structure (Figs. 4D and 5D) starts in the Barents Sea. The arm crosses Scandinavia, Africa (from the Atlases to the Grain Coast), the central Atlantic basin, follows along the Brazilian coast, and disappears in the Drake Passage. The left arm of the Palawan double helix (Figs. 4D and 5D) starts in the Taymyr Peninsula. This crosses Siberia, Gobi, the South China Sea, the Celebes Sea, Australia, and ends in the Tasman Sea. The right arm of the Palawan structure (Figs. 4D and 5D) starts in the Kolyma Range. This crosses the Sea of Okhotsk, Sakhalin, Philippines, the eastern Indian Ocean basin, and disappears in the Kerguelen Plateau.

Table I: Parameters of Global Topographic Helices.

Structure	Left arm		Right arm		Geographical coordinates of arm intersection(s)
	Lengths (km)	Inclination at the equator (°)	Lengths (km)	Inclination at the equator (°)	
Caucasus-Clipperton	55,800	167.5	31,500	12.5	46.4°N, 44.81°E; 5.9°N, 134.7°W
Biscay-Santa Cruz	39,600	162.2	29,800	17.5	44.4°N, 7.3°W; 12.9°S, 171.4°E
Marcus	26,500	150.6	24,900	29.7	21.4°N, 157.5°E
Dakar	17,700	126.9	17,200	53.3	14.9°N, 16.0°W
Palawan	15,400	121.3	15,300	59.5	9.9°N, 119.1°E

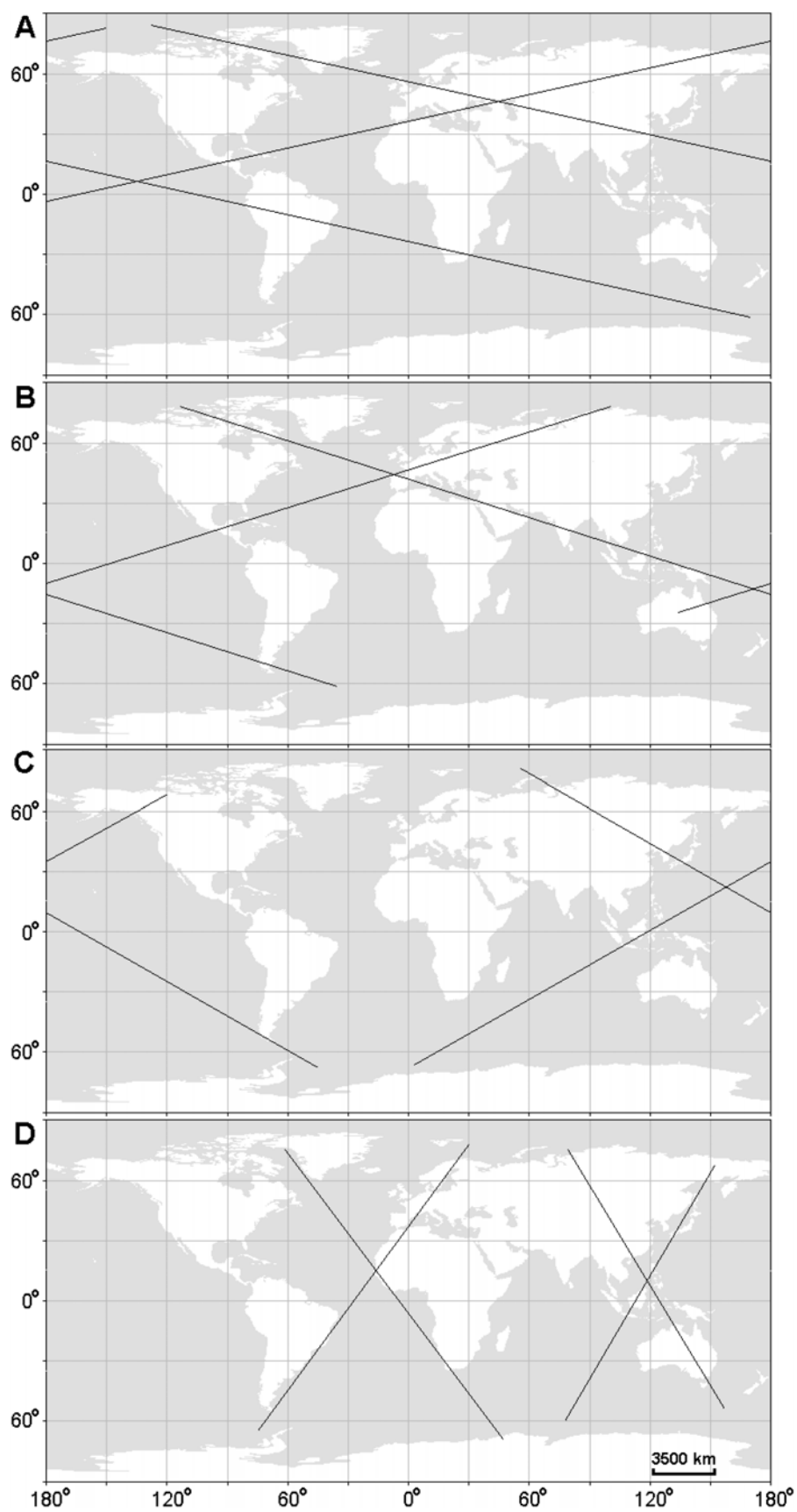


Fig. 4: Global maps of double helical structures: A – Caucasus-Clipperton, B – Biscay-Santa Cruz, C – Marcus, D – Dakar (left) and Palawan (right); the plate carrée projection, 30° graticule.

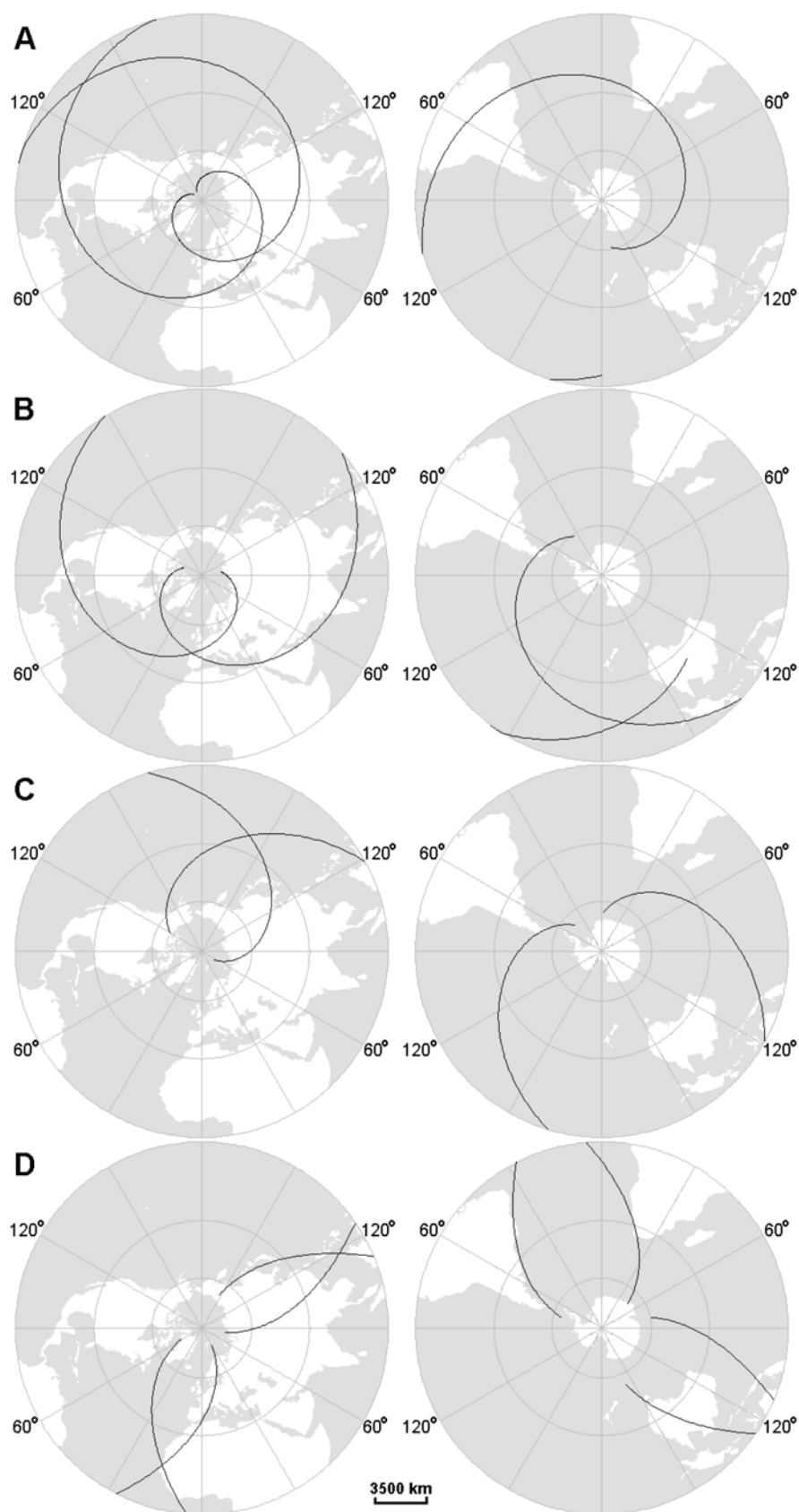


Fig. 5: Maps of double helical structures for the Northern (left) and Southern (right) hemispheres: A – Caucasus-Clipperton, B – Biscay-Santa Cruz, C – Marcus, D – Dakar and Palawan; polar stereographic projections, 30° graticule.

Let us consider previous publications on helical structures of the Earth. First, analysing spatial distribution and preferential directions of actual faults of continental and global scales, Chebanenko (1963) proposed an ideal regular network of the planetary fracturing with a grid size of  $10^\circ$ . Lines of the network had the same inclination at the equator:  $45^\circ$  and  $135^\circ$ . Chebanenko (1963) related the network to lithospheric stresses due to changes in the rotational velocity of the Earth. Second, according to a physical-mathematical model of the torsional deformation of a sphere (Rance, 1968), there are two systems of traces of torsional failure surfaces on the surface of the sphere: shear fractures and cleavage cracks (Rance, 1967). Geometrically, the traces constitute two double helices encircling the sphere from pole to pole (Fig. 6A). The traces vary in inclination at the equator: two mutually symmetrical helices tracing shear fractures are inclined at  $15^\circ$  to  $18^\circ$  and  $165^\circ$  to  $162^\circ$ , and other two helices tracing cleavage cracks are inclined at  $56^\circ$  to  $62^\circ$  and  $124^\circ$  to  $118^\circ$  (Rance, 1967). A search of actual global helical tectonic features resulted in detecting merely several relatively small lineaments referring to faults, trenches, ridges, fracture zones, and seamount chains in basins of the Pacific and Indian Oceans (Rance, 1967, 1969). Subsequently, O'Driscoll (1980) detected two global topographically and tectonically expressed double helical zones by a visual analysis of physiographic maps. The zones had the same inclination at the equator: about  $32^\circ$  and  $160^\circ$  (Fig. 6B). Although O'Driscoll (1980) believed that they are fundamental structural belts governing the global deformation network, shapes of plates, and the planetary evolution, he tried to link these zones with concepts of continental drift and expanding Earth. Finally, Volkov (1995) reported six global double helical structures detected by a visual analysis of physiographic maps. At the equator, three of them were inclined at about  $12^\circ$  and  $168^\circ$ , and other three structures were inclined at about  $22^\circ$  and  $158^\circ$  (Fig. 6C). Volkov (1990, 1995) anticipated that they are traces of tidal effects within the Earth-Moon resonance system of past ages (Alfvén & Arrhenius, 1972). Although the occurrence of planetary resonances in the Solar System is beyond question (Molchanov, 1968; Alfvén & Arrhenius, 1970), the Volkov hypothesis seems to be too exotic.

Let us compare previous publications with our results. The Caucasus-Clipperton double helix (Fig. 4A) coincides with one of the structures reported by Volkov (1995) (Fig. 6C). The left arm of the Biscay-Santa Cruz structure (Fig. 4B) partly agrees with the left arm of one of the helices described by O'Driscoll (1980) (Fig. 6B). A comparison of inclination angles of theoretical traces of torsional deformation (see above), and that of the double helices revealed (Table I) showed that the Caucasus-Clipperton and Biscay-Santa Cruz structures can be assigned to traces of shear fractures, while the Dakar and Palawan structures – to traces of cleavage cracks. The mean deviation of inclination angles of the structures from theoretical values is  $2.8^\circ$ .

Of five double helical structures detected, four have inclination angles fitting theoretical values. This suggests that one may consider topographically expressed helical structures as traces of global torsion. There are several deviations from the theory, such as: (a) arms of each double helix meet off the equator; and (b) there is the double helix, Marcus, with 'abnormal' inclination (Figs. 4, 5, and Table I). The discrepancies between theoretical and observed structures might be in part attributed to the deviation of the Earth's shape from a sphere concerned in the physical-mathematical model by Rance (1968).

The geological manifestation of the double helical structures is unknown. Literature provides some evidence on the geological phenomena related to the structures. For example, there is a wide belt of intensive rock fracturing along the left arm of the Biscay-Santa Cruz structure in Eurasia between  $10^\circ\text{W}$  and  $150^\circ\text{E}$  (Poletaev, 1986). The occurrence of large crystals is observed along a line coaxial with the right arm of the Caucasus-Clipperton structure in Siberia between  $70^\circ\text{E}$  and  $170^\circ\text{W}$  (Evseev, 1993). Large iron and gold ore deposits are located along helical lines and near their intersections (Volkov, 1995). This issue calls for further investigation.

The spatial curves (Fig. 6C) were arbitrarily called 'loxodromes' by Volkov (1990, 1995). To be precise and to avoid confusion, it should be stressed that the lines proposed by Chebanenko (1963), Rance (1968), Volkov (1995), and the author (Figs. 4 and 5) are not loxodromes: none of these spheroidal curves intersects all the meridians at the same angle (Alexander, 2004). Loxodromes are lines detected by O'Driscoll (1980).

The polar stereographic map of the Northern hemisphere (Fig. 5A) presents the Caucasus-Clipperton structure as a nearly ideal plane two-arm Archimedean spiral (Fikhtengolts, 1966, p. 512). Away from the pole, it is approximated by a polar equation  $r = a\theta$ , where  $r$  is a radius,  $\theta$  is an angle, and  $a$  is a constant;  $a = 1.01$ . The left arm of the Caucasus-Clipperton structure can be explicitly described as a spherical Archimedean spiral (Klíma et al., 1981):  $\sigma = R\psi_0\lambda / (2\pi)$ , where  $\sigma$  is a length of a meridian arc between the pole and a point on the spiral ( $\psi$ ,  $\lambda$ ),  $R$  is a radius of the sphere,  $\psi_0$  is a value by which  $\psi$  changes if  $\lambda$  changes by  $2\pi$ ,  $\psi = 0.5\pi - \varphi$ ,  $\varphi$  is the latitude, and  $\lambda$  is the longitude;  $\psi_0 = 79.55^\circ$ . Volkov (2006, personal communication) supposed that all his lines (Fig. 6C) are spherical Archimedean spirals. This issue needs further investigation.

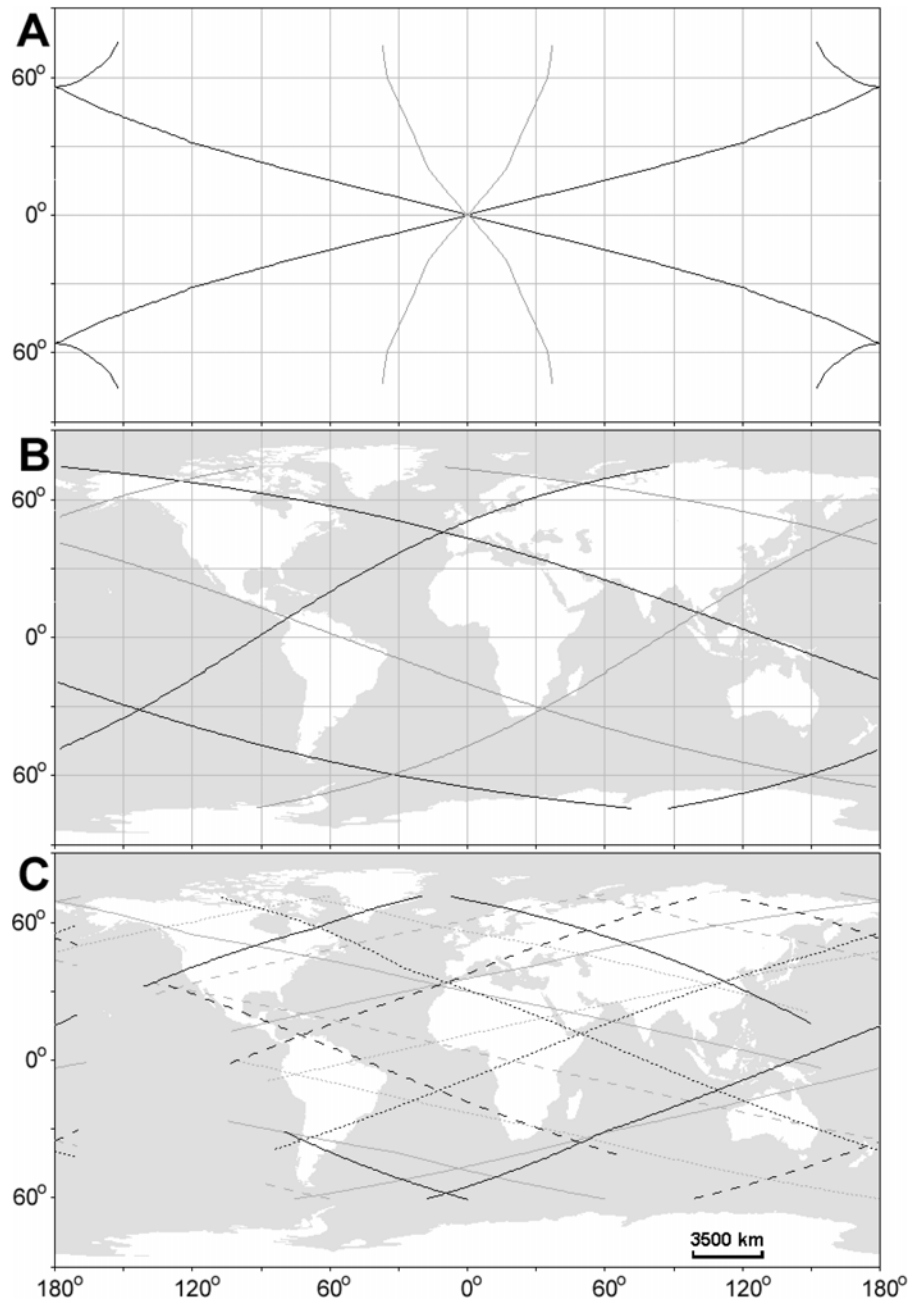


Fig. 6: Schemes of global helices reported previously: A – theoretical traces of torsional deformation of a sphere (Rance, 1967): shear fractures (black) and cleavage cracks (grey); B – axes of two double helical zones (O'Driscoll, 1980); C – six double helices (Volkov, 1995): lines of different colour and style show different double helices. The Mercator projection was used in original publications. To be comparable with the results obtained (Fig. 4), the plate carrée projection is used here, 30° graticule.

### 3.3 Ring Structures

Maps of horizontal, vertical, minimal, maximal, and ring curvatures (Fig. 2A-D, I) were useful to reveal ring structures. One can find some structures on maps of all these variables, while other structures are delineated by a particular topographic attribute. Generally, preliminary results of revealing of circular structures are more ambiguous than that of linear ones.

On the one hand, close inspection of maps of topographic variables led to the detection of about fifty quasi-circular structures (Fig. 7). Twenty of them coincide with ring structures revealed and interpreted before (Table II). Two-thirds of newly founded ring structures are situated within oceanic basins (Fig. 7). This was expected:

in 1970-80s, topographic and physiographic maps used to search ring structures did not include a reasonably accurate bathymetry, while the DEM treated does. In this connection, digital terrain modelling may be useful to search potential impact structures on the seafloor. This is a topical task related to studying the Earth's evolution (Glikson, 1999).

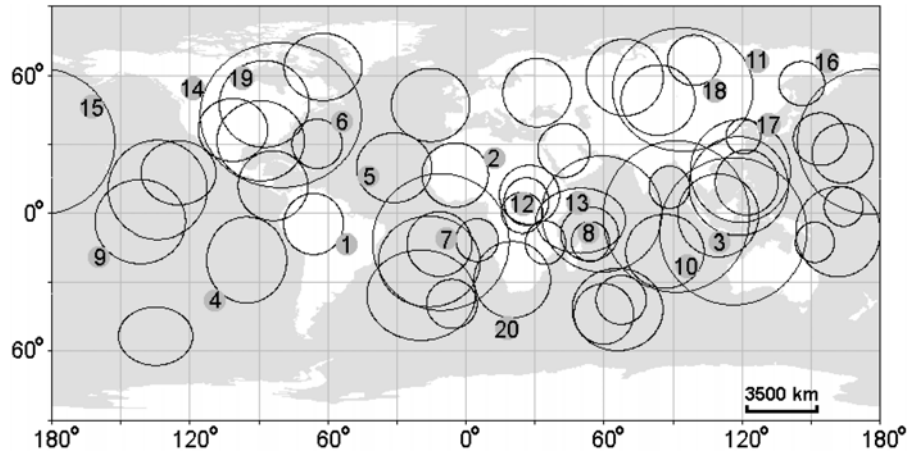


Fig. 7: Global map of ring structures (labelled structures are described in Table II); the plate carrée projection, 30° graticule.

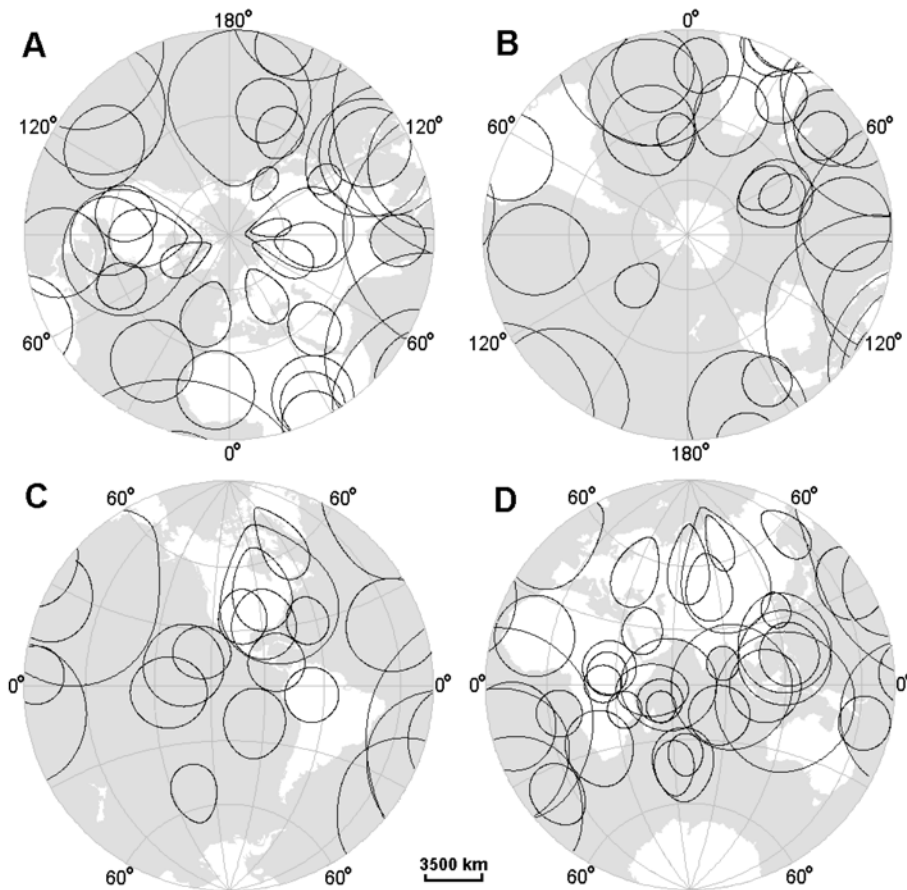


Fig. 8: Maps of ring structures for the Northern (A), Southern (B), Western (C), and Eastern (D) hemispheres; stereographic projections, polar aspects for A and B, and equatorial aspects with central meridians of 110°W and 70°E for C and D, correspondingly; 30° graticule.

Table II: Interpretation <sup>1</sup> of Ring Structures Detected Previously.

Structure (Fig. 8)	Geological interpretations
1	An impact structure (Norman et al., 1977), a Precambrian nuclear (Glukhovsky et al., 1983), a structure with roots in the deep mantle (Ezhov & Khudyakov, 1984).
2	Impact structure (Norman et al., 1977), a Precambrian nuclear (Glukhovsky et al., 1983), a structure with roots in the deep mantle (Ezhov & Khudyakov, 1984), non-interpreted structure (Kats et al., 1989).
3	An impact structure (Norman et al., 1977; Zeilik, 1978), a seismically manifested structure (Poletaev, 1983), a structure with roots in the deep mantle (Ezhov & Khudyakov, 1984), non-interpreted structure (Kats et al., 1989).
4	A seismically manifested structure (Poletaev, 1983), non-interpreted structure (Kats et al., 1989).
5	A seismically manifested structure (Poletaev, 1983).
6	A structure rooted in the deep mantle (Ezhov & Khudyakov, 1984), non-interpreted structure (Kats et al., 1989).
7-10	Non-interpreted structure (Kats et al., 1989).
11, 13	A structure with roots in the deep mantle (Ezhov & Khudyakov, 1984).
12	An impact structure (Zeilik, 1978), a structure with roots in the deep mantle (Ezhov & Khudyakov, 1984).
14, 15	Structures with roots in the upper core (Ezhov & Khudyakov, 1984).
16, 17	An impact structure (Zeilik, 1978).
18-20	A Precambrian nuclear (Glukhovsky et al., 1983).

<sup>1</sup> A ring structure may be differently interpreted by different authors.

On the other hand, properties of map projections may influence results of any research conducted using cartographic data of continental and global scales (Carey, 1988). In particular, this may lead to ‘revealing’ of artificial structures. For the plate carrée projection, shape and area distortions rise from the equator to the poles, with distortion ellipses having major axes in the latitudinal direction (a distortion diagram with Tissot indicatrices can be found elsewhere – Osserman, 2004). A stereographic projection of a sphere holds the shape of circles on the sphere (Bugayevskiy & Snyder, 1995). So, many of structures identified as circles on plate carrée maps of topographic variables (Fig. 7) are not in fact circles (Fig. 8). They resemble the Viviani curve, a result of the intersection of a cylinder with a sphere (Fikhtengolts, 1966, p. 520). Natural, tectonic-driven straining of an original circular structure is possible (i.e., extended craters – Pappalardo & Collins, 2005). However, it is unlikely that these ‘Viviani curves’ are associated with actual geological features, or those geological features are actually manifested on the Earth’s surface as ‘Viviani curves’.

In any case, to identify or refine actual shape and location of structures, a stereographic projection should be used for global maps of topographic variables. This may assist one to separate actual structures and artefacts. The author will explore this issue in the future.

## 4. Conclusions

Eighteen topographic variables were for the first time calculated and mapped for the entire surface of the Earth including both land and seafloor topography. To produce readable and interpretable global maps of topographic attributes, the DEM smoothing was the key step of data pre-processing.

The application of digital terrain modelling provided support for the hypothesis for the existence of double helical structures of the Earth, which are topographically expressed and possibly associated with the torsional deformation of the planet. To understand fully the origin and properties of helical structures (i.e., geological age and depth of manifestation), their comprehensive studies should be conducted. An inclusion of data on global helical structures to plate tectonic models may enhance understanding of the evolution of the Earth.

About fifty quasi-circular structures were detected. Twenty of them coincide with ring structures revealed previously. Two-thirds of newly founded ring structures are situated within oceanic basins. To avoid artefacts due to distortion of map projections, a stereographic projection should be used for global maps of topographic variables intended to reveal ring structures.

This study focused on lineaments and ring structures, but global maps of topographic variables can be useful to study other problems of geology and geophysics (i.e., lithospheric strains and tectonics of planets and satellites of the Solar System).

## References

- [1] Alexander, J. (2004). Loxodromes: A Rhumb Way to Go. *Mathematics Magazine*, 77(5), 349-358.
- [2] Alfvén, H., & Arrhenius, G. (1970). Structure and Evolutionary History of the Solar System, I. *Astrophysics and Space Science*, 8(3), 338-421.
- [3] Alfvén, H., & Arrhenius, G. (1972). Origin and Evolution of the Earth-Moon System. *The Moon*, 5(1-2), 210-230.
- [4] Anderson, D.L. (2002). How Many Plates? *Geology*, 30(5), 411-414.
- [5] Arabelos, D. (2000). Intercomparisons of the Global DTMs ETOPO5, TerrainBase and JGP95E. *Physics and Chemistry of the Earth (A)*, 25(1), 89-93.
- [6] Besprozvanny, P.A., Borodzich, E.V., & Bush, V.A. (1994). Numerical Analysis of Ordering Relations in the Global Network of Lineaments. *Physics of the Solid Earth*, 30(2), 150-159.
- [7] Bugayevskiy, L.M., & Snyder, J. (1995). *Map Projections, A Reference Manual*. London, Taylor & Francis.
- [8] Burbank, D.W., & Anderson, R.S. (2000). *Tectonic Geomorphology*. Malden, Blackwell.
- [9] Bush, V.A. (1983). Transcontinental Lineaments and Problems of Mobilism. *Geotectonics*, 17(4), 271-279.
- [10] Bush, V.A., Bryukhanov, V.N., Kats, Ya.G., & Sulidi-Kondratiev, E.D. (1987). Genetic Types of Ring Structures of Continents. *Bulletin of Moscow Society of Naturalists, Geological Series*, 60(4), 12-23 (in Russian).
- [11] Carey, S.W. (1988). *Theories of the Earth and Universe. A History of Dogma in the Earth Sciences*. Stanford, Stanford University Press.
- [12] Cazenave, A., Souriau, A., & Dominh, K. (1989). Global Coupling of Earth Surface Topography with Hotspots, Geoid and Mantle Heterogeneities. *Nature*, 340(6228), 54-57.
- [13] Chebanenko, I.I. (1962). On Planetary Faults (Lineaments) of Lithosphere. *Dopovidi Akademii Nauk Ukrainy*, (9), 1227-1230 (in Ukrainian, with Russian and English abstracts).
- [14] Chebanenko, I.I. (1963). Principal Regularities of Fault Tectonics of the Earth's crust and Its Problems. Kiev, Ukrainian Academic Press (in Russian).
- [15] Chorowicz, J., Dhont, D., & Gündoğdu, N. (1999). Neotectonics in the Eastern North Anatolian Fault Region (Turkey) Advocates Crustal Extension: Mapping from SAR ERS Imagery and Digital Elevation Model. *Journal of Structural Geology*, 21(5), 511-532.
- [16] Coe, M.T. (1998). A Linked Global Model of Terrestrial Hydrologic Processes: Simulation of Modern Rivers, Lakes, and Wetlands. *Journal of Geophysical Research*, 103(D8), 8885-8899.
- [17] Evseev, A.A. (1993). Siberia's Crystals and Symmetry in the Distribution of Occurrences of Minerals. *World of Stones*, (1), 11-20.
- [18] Ezhov, B.V., & Khudyakov, G.I. (1984). *Structural Geomorphology of Geodynamic Ring Systems: The New Global Concept*. Vladivostok, Far-Eastern Research Centre Press (in Russian).
- [19] Fedorov, A.E. (2003). Once again – Regularities in the Structure of the Earth. In: Fedorov, A.E. (Ed.), *The System of the Planet Earth (Non-Conventional Problems of Geology)*. Papers of the 11<sup>th</sup> Scientific Seminar. Moscow, ROO 'Harmony in Structure of the Earth and Planets', pp. 202-225 (in Russian).
- [20] Fikhtengolts, G.M. (1966). *A Course in Differential and Integral Calculus*, Vol. 1, 6<sup>th</sup> ed. Moscow, Nauka (in Russian).
- [21] Florinsky, I.V. (1992). Recognition of Lineaments and Ring Structures: Quantitative Topographic Techniques. Pushchino, Pushchino Research Centre Press (in Russian, with English abstract).
- [22] Florinsky, I.V. (1996). Quantitative Topographic Method of Fault Morphology Recognition. *Geomorphology*, 16(2), 103-119.
- [23] Florinsky, I.V. (1998a). Combined Analysis of Digital Terrain Models and Remotely Sensed Data in Landscape Investigations. *Progress in Physical Geography*, 22(1), 33-60.
- [24] Florinsky, I.V. (1998b). Derivation of Topographic Variables from a Digital Elevation Model Given by a Spheroidal Trapezoidal Grid. *International Journal of Geographical Information Science*, 12(8), 829-852.
- [25] Florinsky, I.V. (2000). Relationships Between Topographically Expressed Zones of Flow Accumulation and Sites of Fault Intersection: Analysis by Means of Digital Terrain Modelling. *Environmental Modelling and Software*, 15(1), 87-100.
- [26] Florinsky, I.V. (2002). Errors of Signal Processing in Digital Terrain Modelling. *International Journal of Geographical Information Science*, 16(5), 475-501.

- [27] Florinsky, I.V. (2005). Artificial Lineaments in Digital Terrain Modelling: Can Operators of Topographic Variables Cause Them? *Mathematical Geology*, 37(4), 357-372.
- [28] Florinsky, I.V., Grokhilina, T.I., & Mikhailova, N.L. (1995). LANDLORD 2.0: The Software for Analysis and Mapping of Geometrical Characteristics of Relief. *Geodesia i Cartographia* (5), 46-51 (in Russian).
- [29] Glikson, A.Y. (1999). Oceanic Mega-Impacts and Crustal Evolution. *Geology*, 27(5), 387-390.
- [30] GLOBE Task Team and others (Hastings, D.A., Dunbar, P.K., Elphinstone, G.M., Bootz, M., Murakami, H., Maruyama, H., Masaharu, H., Holland, P., Payne, J., Bryant, N.A., Logan, T.L., Muller, J.-P., Schreier, G., & MacDonald, J.S.) (1999). The Global Land One-kilometer Base Elevation (GLOBE) Digital Elevation Model, Version 1.0. Boulder, NOAA, NGDC, [Online]. Available: <http://www.ngdc.noaa.gov/mgg/topo/globe.html>.
- [31] Glukhovskiy, M.Z., Kats, Ya.G., & Moralev, V.M. (1983). On Nuclears of Continents of the World. *Izvestiya Vuzov, Geologia i Razvedka*, (8), 14-19 (in Russian).
- [32] Gosteva, T.S., Patrakova, V.S., & Abramkina, V.A. (1983). Determinating Regularities of Spatial Distribution of Ring Structures using Trend-Analysis of the Topography. *Geologia i Geophysics*, (8), 72-79 (in Russian, with English abstract).
- [33] Jordan, G. (2003). Morphometric Analysis and Tectonic Interpretation of Digital Terrain Data: A Case Study. *Earth Surface Processes and Landforms*, 28(8), 807-822.
- [34] Hastings, D.A., & Dunbar, P.K. (1999). Global Land One-kilometer Base Elevation (GLOBE) Digital Elevation Model, Documentation, Volume 1.0. Key to Geophysical Records Documentation 34. Boulder, NOAA, NGDC, [Online]. Available: <http://www.ngdc.noaa.gov/mgg/topo/globe.html>.
- [35] Kats, Ya.G., & Makarova, N.V. (1985). About a Map of Ring Structures of Continents of the World. *Vestnik Moscovskogo Universiteta, Geology Series*, (6), 32-41 (in Russian).
- [36] Kats, Ya.G., Kozlov, V.V., Poletaev, A.I., & Sulidi-Kondratiev, E.D. (1989). Ring Structures of the Earth: Myth or Reality? Moscow, Nauka (in Russian).
- [37] Katterfeld, G.N., & Charushin, G.V. (1973). General Grid Systems of Planets. *Modern Geology*, 4(4), 253-287.
- [38] Kazanskii, B.A. (2005). Calculation of the Earth's Topography-Related Potential Energy from Digital Data. *Physics of the Solid Earth*, 41(12), 1023-1026.
- [39] Klíma, K., Pick, M., & Pros, Z. (1981). On the Problem of Equal Area Block on a Sphere. *Studia Geophysica et Geodaetica*, 25(1), 24-35.
- [40] Martz, L.W., & de Jong, E. (1988). CATCH: A Fortran Program for Measuring Catchment Area from Digital Elevation Models. *Computers and Geosciences*, 14(5), 627-640.
- [41] McClean, C.J., & Evans, I.S. (2000). Apparent Fractal Dimensions from Continental Scale Digital Elevation Models Using Variogram Methods. *Transactions in GIS*, 4(4), 361-378.
- [42] Meyerhoff, A.A., Taner, I., Morris, A.E.L., Agocs, W.B., Kamen-Kaye, M., Bhat, M.I., Smoot, N.C., & Choi, D.R. (1996). *Surge Tectonics: A New Hypothesis of Global Geodynamics*. Boston, Kluwer.
- [43] Molchanov, A.M. (1968). The Resonant Structure of the Solar System. The Law of Planetary Distances. *Icarus*, 8(1-3), 203-215.
- [44] Moore, I.D., Grayson, R.B., & Ladson, A.R. (1991). Digital Terrain Modelling: A Review of Hydrological, Geomorphological and Biological Applications. *Hydrological Processes*, 5(1), 3-30.
- [45] Moore, R.F., & Simpson, C.J. (1983). Image Analysis - A New Aid in Morphotectonic Studies. In: *Proceedings of the 17<sup>th</sup> International Symposium on Remote Sensing of Environment*, Ann Arbor, 9-13 May 1983, Vol. 3. Ann Arbor, Environmental Research Institute of Michigan, pp. 991-1002.
- [46] Norman, J., Price, N., & Muo, C.-I. (1977). Astrons – The Earth's Oldest Scars? *New Scientist*, 73(1044), 689-692.
- [47] Nyrtsov, M.V. (2000). Developing Map Projections of Actual Surfaces of Celestial Bodies and Methods of Their Study. Abstract of Ph.D. Thesis. Moscow, Moscow State University of Geodesy and Cartography (in Russian).
- [48] O'Driscoll, E.S.T. (1980). The Double Helix in Global Tectonics. *Tectonophysics*, 63(1-4), 397-417.
- [49] Ollier, C. (1981). *Tectonics and Landforms*. London, Longman.
- [50] Osserman, R. (2004). Mathematical Mapping from Mercator to the Millennium. In: Hayes, D.F., & Shubin, T. (Eds.), *Mathematical Adventures for Students and Amateurs*. Mathematical Association of America, pp. 233-257.
- [51] Pappalardo, R.T., & Collins, G.C. (2005). Strained Craters on Ganymede. *Journal of Structural Geology*, 27(5), 827-838.
- [52] Pavlenkova, N.I. (1995). Structural Regularities in the Lithosphere of Continents and Plate Tectonics. *Tectonophysics*, 243(3-4), 223-229.
- [53] Phillips, R.J., Zuber, M.T., Solomon, S.C., Golombek, M.P., Jakosky, B.M., Banerdt, W.B., Smith, D.E., Williams, R.M.E., Hynek, B.M., Aharonson, O., & Hauck, S.A.II. (2001). Ancient Geodynamics and Global-Scale Hydrology on Mars. *Science*, 291(5513), 2587-2591.

- [54] Pike, R.J. (2000). Geomorphometry – Diversity in Quantitative Surface Analysis. *Progress in Physical Geography*, 24(1), 1-20.
- [55] Poletaev, A.I. (1983). Ring Structures of the Earth Derived from Seismic Data. *Izvestiya Vuzov, Geologia i Razvedka*, (8), 159-161 (in Russian).
- [56] Poletaev, A.I. (1986). Seismotectonics of the Main Kopetdag Fault Zone. Moscow, Nauka (in Russian).
- [57] Poletaev, A.I. (1994). Lineament Division of the Earth Crust. Moscow, Geoinformmark (in Russian).
- [58] Pratt, D. (2000). Plate Tectonics: A Paradigm Under Threat. *Journal of Scientific Exploration*, 14(3), 307-352.
- [59] Rance, H. (1967). Major Lineaments and Torsional Deformation of the Earth. *Journal of Geophysical Research*, 72(8), 2213-2217.
- [60] Rance, H. (1968). Plastic Flow and Fracture in a Torsionally Stressed Planetary Sphere. *Journal of Mathematics and Mechanics*, 17(10), 953-974.
- [61] Rance, H. (1969). Lineaments and Torsional Deformation of the Earth: Indian Ocean. *Journal of Geophysical Research*, 74(12), 3271-3272.
- [62] Renssen, H., & Knoop, J.M. (2000). A Global River Routing Network for Use in Hydrological Modeling. *Journal of Hydrology*, 230(3-4), 230-243.
- [63] Scheidegger, A.E. (2004). *Morphotectonics*. Berlin, Springer.
- [64] Schowengerdt, R.A. & Glass, C.E. (1983). Digitally Processed Topographic Data for Regional Tectonic Evaluations. *Geological Society of America Bulletin*, 94(4), 549-556.
- [65] Shary, P.A., Sharaya, L.S., & Mitusov, A.V. (2002). Fundamental Quantitative Methods of Land Surface Analysis. *Geoderma*, 107(1-2), 1-32.
- [66] Smith, D.E., Zuber, M.T., Neumann, G.A., & Lemoine, F.G. (1997). Topography of the Moon from the Clementine Lidar. *Journal of Geophysical Research*, 102(E1), 1591-1611.
- [67] Smith, D.E., Zuber, M.T., Solomon, S.C., Phillips, R.J., Head, J.W., Garvin, J.B., Banerdt, W.B., Muhleman, D.O., Pettengill, G.H., Neumann, G.A., Lemoine, F.G., Abshire, J.B., Aharonson, O., Brown, C.D., Hauck, S.A., Ivanov, A.B., McGovern, P.J., Zwally, H.J., & Duxbury, T.C. (1999). The Global Topography of Mars and Implications for Surface Evolution. *Science*, 284(5419), 1495-1503.
- [68] Smith, W.H., & Sandwell, D.T. (1997). Global Sea Floor Topography from Satellite Altimetry and Ship Depth Soundings. *Science*, 277(5334), 1956-1962.
- [69] Smoot, N.C. (1997). Aligned Buoyant Highs, Across-Trench Deformation, Clustered Volcanoes, and Deep Earthquakes are not Aligned with Plate-Tectonic Theory. *Geomorphology*, 18(3-4), 199-222.
- [70] Smoot, N.C. (2001). Earth Geodynamic Hypotheses Updated. *Journal of Scientific Exploration*, 15(3), 465-494.
- [71] Storetvedt, K.M. (2003). *Global Wrench Tectonics: Theory of Earth Evolution*. Bergen, Fagbokforlaget.
- [72] Tobler, W.R. (1967). Of Maps and Matrices. *Journal of Regional Science*, 7(2 Suppl.), 275-280.
- [73] Trifonov, V.G., Makarov, V.I., Safonov, Yu.G., & Florensky, P.V. (Eds.) (1983). *Space Remote-Sensing Data in Geology*. Moscow, Nauka (in Russian, with English contents).
- [74] U.S. Department of Commerce, National Oceanic and Atmospheric Administration, National Geophysical Data Center (2001). 2-minute Gridded Global Relief Data (ETOPO2), [Online]. Available: <http://www.ngdc.noaa.gov/mgg/fliers/01mgg04.html>
- [75] USSR General Headquarters, Department of Military Topography, 1984. *Atlas of Officer*. Moscow, Department of Military Topography (in Russian).
- [76] Volkov, Yu.V. (1990). Solar Activity and Climatic Zonality. *Bulletin of Moscow Society of Naturalists, Geological Series*, 65(3), 108-115 (in Russian, with English abstract).
- [77] Volkov, Yu.V. (1995). Loxodromy and Minerageny (Influence of Astronomic Resonances in the Earth-Moon System on the Origin of Ore Deposits in the Earth Crust). *Bulletin of Moscow Society of Naturalists, Geological Series*, 70(6), 90-94 (in Russian, with English abstract).
- [78] Vörösmarty, C.J., Fekete, B.M., Meybeck, M., & Lammers, R.B. (2000). Geomorphometric Attributes of the Global System of Rivers at 30-minute Spatial Resolution. *Journal of Hydrology*, 237(1-2), 17-39.
- [79] Wise, D.U. (1982). Linesmanship and the Practice of Linear Geo-Art. *Geological Society of America Bulletin*, 93(9), 886-888.
- [80] Zeilik, B.S. (1978). On the Origin of Arched and Ring Structures on the Earth and Other Planets: Impact-Explosive Tectonics. Moscow, VIEMS (in Russian).

## Acknowledgements

Author thanks V.G. Trifonov, A.E. Fedorov, A.I. Poletaev, Yu.V. Volkov, and H. Rance for discussions.